

Research Article

Devesh Bharadwaj, Thomas M. Fyles and Henning Struchtrup* Multistage Pressure-Retarded Osmosis

DOI 10.1515/jnet-2016-0017

Received March 7, 2016; revised May 18, 2015; accepted May 27, 2016

Abstract: One promising sustainable energy source is the chemical potential difference between salt and freshwater. The membrane process of pressure-retarded osmosis (PRO) has been the most widely investigated means to harvest salinity gradient energy. In this report, we analyse the thermodynamic efficiency of multi-stage PRO systems to optimize energy recovery from a salinity gradient. We establish a unified description of the efficiencies of the component pumps (P), turbines (T), pressure exchangers (PX), and membrane modules (M) and exploit this model to determine the maximum available work with respect to the volume of the brine produced, the volume of the sea water consumed, or the volume of the freshwater that permeates the membrane. In an idealized series configuration of 1–20 modules (P – M – T), the three optimization conditions have significantly different intermediate operating pressures in the modules, but demonstrate that multistage systems can recover a significantly larger fraction of the available work compared to single-stage PRO. The biggest proportional advantage occurs for one to three modules in series. The available work depends upon the component efficiencies, but the proportional advantage of multistage PRO is retained. We also optimize one- and two-stage PX– M – T and P – M – T configurations with respect to the three volume parameters, and again significantly different optimal operating conditions are found. PX– M – T systems are more efficient than P – M – T systems, and two-stage systems have efficiency advantages that transcend assumed component efficiencies. The results indicate that overall system design with a clear focus on critical optimization parameters has the potential to significantly improve the near-term practical feasibility of PRO.

Keywords: pressure-retarded osmosis, renewable energies, pressure exchangers

1 Introduction

The global energy resource represented by mixing freshwater into seawater is about 2 TW or approximately 10 % of global energy demand [1]. Although the resource potential was recognized half a century ago [2] and attracted attention in the 1970s [3–5], the required innovations to overcome technological limitations are only now emerging [6]. Salinity-gradient power generation by pressure-retarded osmosis (PRO) or reverse electrodialysis (RED) are membrane technologies that potentially could harvest this resource [7]. As a prelude to commercialization, a 10 kW pilot-scale PRO power plant was designed and operated by Statkraft from 2009 to 2012. The plant was based on a single-stage design with a pressure exchanger for energy recovery. The design anticipated membranes capable of producing 5 W/m² from a seawater–freshwater gradient at a hydraulic pressure of half the osmotic pressure difference. This power density has not yet been achieved in a commercial membrane. The closure of the Statkraft plant is linked to membrane inefficiencies and power generation economics at commercial scale, rather than to other design factors [8].

The barriers to the development of PRO-based power generation have been widely analysed, starting with an early discussion [9] of the required membrane structural characteristics and their influence on power density [6, 10]. Membrane power density directly controls the overall economic feasibility of PRO-generated power [1, 6], and the development of thin, high-strength membrane materials capable of

*Corresponding author: Henning Struchtrup, Department of Mechanical Engineering, University of Victoria, Victoria, BC, Canada, E-mail: struchtr@uvic.ca

Devesh Bharadwaj, Department of Mechanical Engineering, University of Victoria, Victoria, BC, Canada, E-mail: devesh@uvic.ca

Thomas M. Fyles, Department of Chemistry, University of Victoria, Victoria, BC, Canada, E-mail: tmf@uvic.ca

high water flux and good salt rejection is one of the critical technological barriers to efficient commercial-scale PRO [1, 6, 8, 10, 11]. The economic and energetic feasibility of PRO-based power also critically depends on pumping and pre-treatment costs which may exceed the energy available from the resource [11–13].

The work available in PRO is proportional to the osmotic pressure difference across the membrane. This observation has led to proposals to use more concentrated brines such as that occur in saline aquifers or the Dead Sea [14], or in the brines produced in reverse osmosis (RO) desalination, in place of seawater [15, 16]. A pilot-scale implementation using the salinity gradient between the concentrated end brine of an RO desalination plant and product water from a domestic wastewater treatment facility achieved a maximum power density of 7.7 W/m^2 at 38% permeation of water into brine, although fouling from the freshwater source ultimately shortened the practical membrane lifetime [17]. Even higher osmotic pressures are accessible in closed-loop systems that use low-grade heat to regenerate the draw solution; examples are the ammonia–carbon dioxide osmotic heat engine [18], hybrid PRO-membrane distillation systems [19, 20], or the use of a hydroacid complex draw solution in a closed loop with regeneration as draw solution, and low salinity freshwater as feed solution [21].

Virtually, all analysis and modelling of PRO [12, 22–28] has been based on a single-stage constant-pressure PRO system (Figure 1) [6, 11]. In this configuration, a membrane module (or series array) is fed with pressurized saltwater at a set hydrostatic pressure. Although counterflow configurations have been considered [12], the more common design is the same direction of fresh and seawater flow through the module. In this “co-flow” configuration, the osmotic gradient is high at the membrane inlet, and gradually decreases along the membrane length coordinate. A relatively large portion of the water flows across the near-inlet part of the membrane, and less across the near-outlet section. From a thermodynamic viewpoint, the entropy generation is proportional to the square of the driving force [29]; hence, there is large entropy generation at the near-inlet part of the membrane. Since entropy generation decreases work output, this implies inefficient use of the membrane. Counterflow designs can partially mitigate the work decrease, but the central issue is that the single-pressure design enforces inefficient use of the resource.

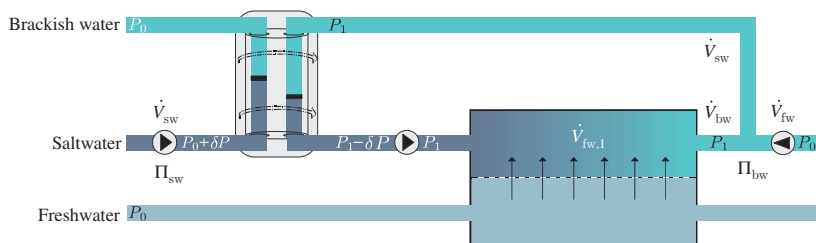


Figure 1: Standard configuration for pressure-retarded osmosis (PRO): saltwater, pressurized in a pressure exchanger, draws freshwater across a semipermeable membrane. The resulting flow is split into a flow to the pressure exchanger, and a flow to a turbine where work is produced. A feed and a booster pump are required to compensate for pressure losses.

We consider alternative configurations for PRO systems that use multistage designs that could allow to extract more of the available energy via the use of different pressures. In this context, we point out that multistage configurations are well known in thermodynamic applications such as air compressors, gas turbines, advanced steam and cooling cycles, where they are beneficial due to the reduced entropy generation [29, 30]. All practical multistage systems have more complex process designs and require additional components that reduce the fundamental advantages but do not render them impractical. Our analysis here is focussed on exploring the inherent advantages – if any – to multistage PRO with the expectation that subsequent and more sophisticated analysis of favourable designs will establish if the added complexity and real-world limitations overwhelm any inherent advantages there might be. However, “multistage” does not imply a single design so we are initially interested in which configuration offers the largest fundamental advantage. Once we have a sense of where the advantage may lie, we can shift towards more realistic analyses.

The question is: what simplifications can we make at the outset that will facilitate the analysis while preserving essential practical elements? We assume below that all efficiency reducing factors within the membrane modules due to reverse salt flux, internal concentration polarization, module design, fouling, etc. can all be reduced to a focus on how much of the available input chemical potential is harvested at the membrane outlet.

Our approach is thermodynamic, similar to endoreversible thermodynamics [31], so our focus is on intensive properties of the system (pressure, salt concentration) rather than on extensive properties (membrane area). We recognize that both these simplifying assumptions will be abandoned on the way to practical systems. Our goal in this initial analysis is to discover if multistage PRO has any inherent advantage relative to the single-stage and constant pressure systems that have been explored by previous studies.

First, for proof of concept, we consider a series of membrane units and turbines with optimized intermediate pressures. It will be seen that an increase of stages leads to increased power generation. For practical applications, a very large number of stages will not be feasible. Therefore, for the second part of the paper, we evaluate three different two-stage configurations. Apart from membranes, PRO systems require mechanical devices like pumps, turbines, and pressure exchangers, to increase and lower pressures and to generate power. The overall system performance depends in part on the efficiency of the mechanical devices. Since pressure exchangers are more efficient than turbine–pump pairs, they are considered as a standard element of PRO systems (Figure 1) [1, 6, 8].

For single-stage or multistage systems, system performance depends strongly on the choice of membrane pressures, which must be obtained from an optimization procedure. The pressures in the different configurations will be optimized for power output per expenditure, where different expenditures are considered. For the energy production of mixing seawater and river water, we already understand the importance and necessity of energy output per membrane area which directly relates to plant scale and capital cost. From a thermodynamic perspective, the power density is not fundamental but depends upon case-specific membrane properties. The fundamental issue is the ability of the membrane module to extract the work from the input streams. As a consequence, we seek to optimize PRO performance for a given membrane effectiveness based on the input and output streams. For places with limited freshwater availability the focus might be on maximum work per volume of freshwater drawn, or for locations with constraints on plant size, one will be interested in maximum work per volume of total water discharged. The saline draw solution might be considered as the limiting resource, as in the case of ammonia–carbon dioxide-based draw solutions for power production or where pre-treatment costs are significant [8, 18]. In this case, the system would be optimized to produce maximum work per volume of draw solution utilized.

For the evaluation of the configurations, we consider a classical thermodynamic approach, where standard elements – membrane unit, pump, turbine, pressure exchanger – are described by meaningful efficiency measures. The overall performance of the system can then be determined in dependence of the efficiencies of its elements. Here, we use standard definitions for the efficiencies of pumps, turbines, and pressure exchangers. To be able to incorporate membrane modules into this description, we define a membrane module effectiveness (Section 2.4). This approach is general and is consistent with incorporation of more sophisticated membrane and module-level transport models at subsequent stages. Here we are solely concerned with the potential of different multistage PRO system designs to extract the maximum work as defined by the three flows to and from the system as a whole.

2 Efficiencies of thermodynamic components

As stated above, we shall consider PRO systems that are composed of only four different components: pumps, turbines, pressure exchangers, and membrane modules. The various systems will be analysed based on the thermodynamic efficiencies of their components, which we will define in this section, after stating some general assumptions and relations that will be used in the sequel.

Subsequently, all flows – freshwater, saltwater, and brackish water – are considered as incompressible liquids, with no change of volume in mixing. All salt solutions are assumed to be sufficiently dilute, so that the osmotic pressure of a solution α can be approximated as

$$\Pi_{\alpha} = ic_{\alpha}\bar{R}T, \quad (1)$$

where i is the Van't Hoff factor, which accounts for the number of individual particles of a compound dissolved in solution, and c is the molar concentration of the solution (unit: mol/L). Furthermore, $\bar{R} = 8.314$ kJ/(kmol K) is the universal gas constant, and T is the thermodynamic temperature of the solution (unit: K).

One litre of typical seawater (sw) contains about 35 g of NaCl and 993 g of freshwater, which implies a molar concentration $c_{sw} = 0.6$ mol/L. Since NaCl dissociates into Na^+ and Cl^- ions, the Van't Hoff factor is $i = 2$, giving the osmotic pressure of seawater at 280.65 K (75 °C) as $\Pi_{sw} = 28$ bar [29].

When a volume flow \dot{V}_{sw} (unit: L/s) of saltwater with concentration c_{sw} is mixed with a volume flow \dot{V}_{fw} of freshwater, the resulting brackish water (bw) has volume flow $\dot{V}_{bw} = \dot{V}_{sw} + \dot{V}_{fw}$, and the concentration

$$c_{bw} = c_{sw} \frac{\dot{V}_{sw}}{\dot{V}_{bw}} = c_{sw} \frac{\dot{V}_{sw}}{\dot{V}_{sw} + \dot{V}_{fw}}. \quad (2)$$

The last equation implies that the ratio of osmotic pressures of incoming saltwater (Π_{sw} , \dot{V}_{sw}) and exiting brackish water (Π_{bw} , \dot{V}_{bw}) is simply given by the volume flow ratio:

$$\frac{\Pi_{bw}}{\Pi_{sw}} = \frac{\dot{V}_{sw}}{\dot{V}_{bw}} = \frac{\dot{V}_{sw}}{\dot{V}_{sw} + \dot{V}_{fw}}. \quad (3)$$

2.1 Pumps and turbines

To describe irreversible losses in pumps (P) and turbines (T), we use isentropic efficiencies [29]. The pump work required to pressurize a volume flow \dot{V} of an incompressible liquid from hydraulic pressure P_L to P_H is (power, i. e. work per unit time)

$$\dot{W}_P = \frac{1}{\eta_P} \dot{V}(P_L - P_H), \quad (4)$$

where η_P is the isentropic efficiency of the pump. For a fully reversible pump $\eta_P = 1$, while for irreversible pumps $0 < \eta_P < 1$. Note that the pump work is negative, which implies that power must be provided to run the pump.

Similarly, the turbine work extracted from a volume flow \dot{V} depressurizing from pressure P_H to P_L is (power)

$$\dot{W}_T = \eta_T \dot{V}(P_H - P_L), \quad (5)$$

where η_T is the isentropic efficiency of the turbine. For a fully reversible turbine $\eta_T = 1$, while for irreversible turbines $0 < \eta_T < 1$.

Actual turbine and pump efficiencies depend on the construction as well as on size, with larger devices usually having larger efficiencies. Excellent devices reach efficiencies around 90%, and we shall use this upper value for our simulations.

For comparison with pressure exchangers, we consider a turbine–pump pair, where both devices are passed by the same volume flow \dot{V} , and cover the same pressure difference ($P_H - P_L$). Such a pair leads to exchange of pressure between the pump flow, which is pressurized, and the turbine flow, which is depressurized. Since the pump requires more work than the turbine delivers, the net work requirement $\delta\dot{W}_{TP}$ for the pair is (power, defined as positive).

$$\delta\dot{W}_{TP} = |\dot{W}_T + \dot{W}_P| = \left(\frac{1}{\eta_p} - \eta_T\right) \dot{V}(P_H - P_L) = \gamma_{TP} \dot{V}(P_H - P_L), \quad (6)$$

where we have defined the loss factor $\gamma_{TP} = \left(\frac{1}{\eta_p} - \eta_T\right)$, which can assume values above 1.

Obviously, the work requirement vanishes for a fully reversible system, where $\eta_p = \eta_T = 1$ and $\gamma_{TP} = 0$, while for the typical values $\eta_p = \eta_T = 0.9$ the loss factor is $\gamma_{TP} = 21\%$. We note in particular that the net work requirement for the pair is proportional to the pressure difference $(P_H - P_L)$.

2.2 Pressure exchanger

Pressure exchangers (PX) aim at direct pressure transfer between a high-pressure stream and a low-pressure stream. These devices are proven to have higher energy recovery efficiency than turbine–pump combinations [32]. Pressure exchangers are routinely used in RO plants for freshwater production [33–35] and are part of all existing, planned, or suggested PRO plants [1, 6, 8].

Typically, pressure exchangers use flow channels in a rotating drum, so that the channels are sometimes in contact with the low-pressure flows, and sometimes with the high-pressure flows, as sketched in Figure 2. When a channel arrives at low pressure, it is filled with liquid I and brought into contact with liquid II at pressure $P_L + \delta P_L$ on one side, and liquid I at pressure P_L at the other side. Due to the pressure difference δP_L , liquid I is replaced by liquid II, that is liquid I is pushed out at pressure P_L . Now the rotating drum brings the channel, filled with liquid II, into contact with the high-pressure streams. Liquid I at pressure P_H enters the channel while liquid II is pushed out at pressure $P_H - \delta P_H$.

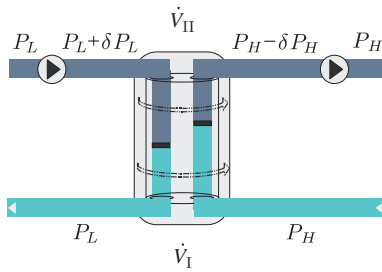


Figure 2: Flows and pressures for a pressure exchanger involving incoming streams with volume flows \dot{V}_I and \dot{V}_{II} at pressures P_H and P_L , respectively. A feed and a booster pump are required to overcome the pressure differences δP_L and δP_H for filling and discharge; leakage flow is not explicitly shown.

Figure 2 shows schematically the incoming and outgoing flows, and the corresponding pressures, where pressure is to be exchanged between the high-pressure flow \dot{V}_I at P_H and the low-pressure flow \dot{V}_{II} at $P_L + \delta P_L$. Due to irreversibilities, pressure exchange is not perfect, so that \dot{V}_{II} leaves at $P_H - \delta P_H$, while \dot{V}_I leaves at $P_L = (P_L + \delta P_L) - \delta P_L$, where δP_H and δP_L are the irreversible pressure losses. Due to leakage between the streams, the flow rates might change by $\delta\dot{V}_L$ in either direction.

The pressure differences δP_H and δP_L are required to ensure flow in charge and discharge, that is they relate mainly to hydrodynamic losses. While in pumps and turbines work loss is proportional to the pressure difference, the pressure loss δP in pressure exchangers does not depend on the pressure difference, but can be considered as constant. According to information from Energy Recovery Inc. (ERI) [36], in the relevant pressure ranges typical pressure loss for both streams is approximately $\delta P_L = \delta P_H = \delta P = 0.5$ bar, and we shall use this value for our modelling below.

Since the liquids replace each other in charge/discharge, it is required that the volume flow rates for the two entering streams are equal, $\dot{V}_I = \dot{V}_{II}$. Some pressure exchangers, e. g. those made by ERI [36], use a small amount of leakage to ensure lubrication, but generally leakage is small. In the present context, leakage can be ignored, hence we set $\delta\dot{V}_L = 0$.

Because of the pressure losses δP_L , δP_H the exchange of pressures between the two streams is not perfect. To correct for the losses, feed and booster pumps are required, as indicated in Figure 2, which together require the total work input

$$\delta\dot{W}_{PX} = (\delta P_L + \delta P_H)\dot{V} = 2\delta P\dot{V}. \quad (7)$$

Using the above definition (6), we find the loss factor for a pressure exchanger as

$$\gamma_{PX} = \frac{\delta\dot{W}_{PX}}{\dot{V}(P_H - P_L)} = \frac{2\delta P}{P_H - P_L}. \quad (8)$$

With the pressure loss being approximately constant, the loss factor decreases significantly with increasing pressure difference. Hence, pressure exchangers are particularly useful at large pressure differences. They are routinely used in RO plants, which operate with pressure differences of ~ 60 bar, so that – with the above data – the loss factor is only 1.7%. For a typical PRO plant, the pressure is about 15 bar, corresponding to a loss factor of 6.7%.

For smaller pressure differences, pressure exchangers lose the advantage against turbine–pump pairs, e. g. for the data above, when the pressure difference is below 4.7 bar, the loss factor is larger than the loss factor for a turbine–pump pair with efficiencies of $\eta_T = \eta_P = 0.9$.

As the above discussion shows, the use of the loss factor allows a good comparison of pressure exchangers and turbine–pump pairs. We shall now briefly discuss the typical definition of pressure exchanger efficiency, as the ratio between the overall energy flows exiting and entering, that is (with $\dot{V}_I = \dot{V}_{II}$, $\delta P_H = \delta P_L$, $\delta\dot{V}_L = 0$) [33],

$$\eta_{PX} = \frac{\dot{V}_I(P_L - \delta P_L) + \dot{V}_{II}(P_H - \delta P_H)}{\dot{V}_I P_H + \dot{V}_{II} P_L} = 1 - \frac{2\delta P}{P_H + P_L}. \quad (9)$$

This definition assigns a larger efficiency for cases where both flows have higher absolute pressures P_H, P_L , but the same pressure difference $P_H - P_L$. Clearly, this cannot be justified for flows of (quasi-)incompressible liquids, for which efficiency should depend on the net forces required, which are pressure differences. Hence, we recommend to not use the above misleading efficiency η_{PX} but rather the loss factor γ_{PX} to evaluate the quality of a pressure exchanger. The loss factor properly relates exchanger performance to pressure differences ($\delta P, P_H - P_L$), and thus is independent of pressure increases that leave the difference unchanged.

At first glance, one might consider defining an alternative PX efficiency as $\hat{\eta}_{PX} = 1 - \gamma_{PX}$. This, however, would be improper, since the loss factor γ_{PX} might assume values above unity, hence $\hat{\eta}_{PX}$ is not limited to $(0, 1)$.

2.3 Membrane module

In a PRO system, the membrane module draws freshwater across the membrane into pressurized saltwater, to produce a larger stream of pressurized brackish water.

Figure 3 shows the relevant flows of a membrane module. A volume flow \dot{V}_{sw} of saltwater with osmotic pressure Π_{sw} (concentration c_{sw}) enters the module at pressure P_H , where $P_H - P_0 < \Pi_{sw}$. As it flows along the membrane, osmotic forces draw freshwater across the membrane, which mixes with the saltwater; the total flow of freshwater drawn across the membrane is \dot{V}_{fw} . The resulting brackish water leaves with reduced concentration, increased volume flow $\dot{V}_{bw} = \dot{V}_{sw} + \dot{V}_{fw}$, and reduced osmotic pressure $\Pi_{bw} < \Pi_{sw}$. We ignore the loss of hydraulic pressure due to friction, so that the exiting brackish water is at pressure P_H . The freshwater on the other side of the membrane is at pressure P_0 .

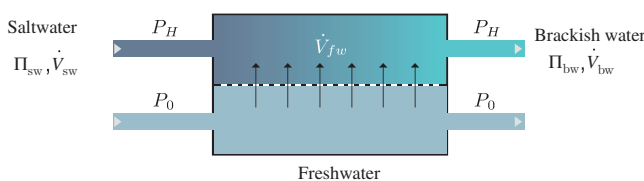


Figure 3: Flows and pressure for a PRO membrane module. Pressurized saltwater of osmotic pressure Π_{sw} draws freshwater across the membrane. The resulting brackish water has a lower osmotic pressure $\Pi_{bw} < \Pi_{sw}$. Pressure losses in the module are ignored.

In real membranes, a small amount of salt passes through the membrane from the saltwater to the freshwater side – this is ignored in our discussion.

Following thermodynamic tradition, we define membrane effectiveness as the ratio of actual performance over best-case performance. In the best case, the membrane module will allow for complete equilibration across the membrane at the end of the module. This implies that in the perfectly effective module the exiting osmotic pressure is just the hydraulic pressure difference between freshwater and saltwater:

$$\Pi_{\text{bw}}^{\text{eq}} = \Delta P = P_H - P_0; \quad (10)$$

this reflects the definition of osmotic pressure as an equilibrium quantity.

We base the effectiveness on the difference in osmotic pressures between inlet and outlet, which in the perfect module is $\Pi_{\text{sw}} - \Pi_{\text{bw}}^{\text{eq}} = \Pi_{\text{sw}} - \Delta P$. Perfect equilibration requires long time, and in membrane modules of finite length, the saltwater flow will not spend enough time to equilibrate. Hence, less freshwater will be drawn across the membrane, and the osmotic pressure of the exiting flow will be above the equilibrium value, $\Pi_{\text{bw}} > \Pi_{\text{bw}}^{\text{eq}} = \Delta P$. A meaningful membrane module effectiveness can be defined as

$$\eta_{\text{MM}} = \frac{\Pi_{\text{sw}} - \Pi_{\text{bw}}}{\Pi_{\text{sw}} - \Pi_{\text{bw}}^{\text{eq}}} = \frac{\Pi_{\text{sw}} - \Pi_{\text{bw}}}{\Pi_{\text{sw}} - \Delta P}. \quad (11)$$

We note that $\eta_{\text{MM}} = 1$ for a perfect module, and $\eta_{\text{MM}} = 0$ in case that no freshwater passes the membrane. Later, we will use the module effectiveness to determine the exit stream osmotic pressure in a membrane module, as

$$\Pi_{\text{bw}} = (1 - \eta_{\text{MM}})\Pi_{\text{sw}} + \eta_{\text{MM}}\Delta P; \quad (12)$$

the amount of freshwater drawn can then be determined from eq. (3), as

$$\dot{V}_{\text{fw}} = \dot{V}_{\text{sw}} \left(\frac{\Pi_{\text{sw}}}{\Pi_{\text{bw}}} - 1 \right) = \dot{V}_{\text{sw}} \frac{\Pi_{\text{sw}} - \Delta P}{\left(\frac{1}{\eta_{\text{MM}}} - 1 \right) \Pi_{\text{sw}} + \Delta P}. \quad (13)$$

Straub et al. [24] considered the performance of modules at different conditions. From their results, one can easily conclude that there is not a single value of effectiveness that describes a module, but rather that the module effectiveness depends on operating conditions. To estimate what values seem to be realistic, we consider data from Ref. [14], where the author modelled a large-scale PRO plant with a Filmtec composite BW-30 brackish water membrane, a 25 bar osmotic pressure salt solution fed into the membrane at a hydraulic pressure of 12.2 bar to find the exiting brackish water stream at an osmotic pressure of 18 bar [14]. With the particular membrane characteristics, membrane module size, and volumetric flow rates given in Ref. [14], the membrane module efficiency is obtained as $\eta_{\text{MM}} = 0.55$.

The above approach to module effectiveness treats the module as a black box without a particular focus on any membrane property, form factor, or flow characteristics. The value of this approach is that it allows rigorous analysis of the system performance with respect to an ideal case. Subsequent, more detailed and sophisticated analyses may provide deeper insights into the key factors that influence module effectiveness.

Some additional comments are in order: In working membrane modules, there will be a non-equilibrium between the saltwater and freshwater flows throughout the membrane unit, that is $\Pi_{\text{sw}} > \Delta P$. Indeed, this non-equilibrium is the driving force for the freshwater flow across the membrane, which is proportional to the pressure imbalance, so that the flow through a membrane area element dA is $d\dot{V}_{\text{fw}} = \alpha(\Pi_{\text{sw}} - \Delta P)dA$, where α is membrane permeability. The corresponding entropy generation for the module is determined in Appendix, eq. (36) with $P_{\text{fw}} = P_0$, $\dot{W} = 0$, as

$$T\dot{S}_{\text{gen}} = \dot{V}_{\text{sw}} \left[\Pi_{\text{sw}} \ln \left(1 + \frac{\dot{V}_{\text{fw}}}{\dot{V}_{\text{sw}}} \right) - \frac{\dot{V}_{\text{fw}}}{\dot{V}_{\text{sw}}} \Delta P \right], \quad (14)$$

where \dot{V}_{fw} must be inserted from eq. (13). We only show the result for not too large pressure deviations (i. e. small freshwater flow), which follow from expansion as

$$T\dot{S}_{gen} = (2 - \eta_{MM}) \frac{\eta_{MM}}{2} \frac{\dot{V}_{sw}}{\Pi_{sw}} (\Pi_{sw} - \Delta P)^2 + \mathcal{O}((\Pi_{sw} - \Delta P)^3). \quad (15)$$

Hence, entropy generation in the module is quadratic (to leading order) in the pressure difference $(\Pi_{sw} - \Delta P)$. This is similar to heat transfer over a finite temperature difference ΔT , where heat transfer rate is proportional to ΔT , and the entropy generation is proportional to ΔT^2 . Indeed, the module effectiveness (11) is defined similarly to the heat exchanger effectiveness [37]. With the above definition (11), all modules are irreversible, even if their effectiveness is unity. A module will be more effective and produce less entropy, when the pressure imbalance $(\Pi_{sw} - \Delta P)$ at inflow is smaller.

3 *n*-Stage PRO system

3.1 The case for multistage PRO

Standard PRO systems consist of a single membrane module, pressure exchanger, and turbine as depicted in Figure 1. Saltwater of osmotic pressure Π_{sw} is pressurized from P_0 to $P_H = P_0 + \Delta P$, and brought into contact with freshwater in the membrane module so that the flow \dot{V}_{fw} is drawn across. The work that can be obtained from this set-up is at best $\dot{W}_{best} = \dot{V}_{fw} \Delta P = \hat{\alpha} (\Pi_{sw} - \Delta P) \Delta P$, where $\hat{\alpha}$ is a suitable average membrane permeability. This work becomes maximum for $\Delta P = \frac{1}{2} \Pi_{sw}$, for which $\dot{W}_{best, max} = \frac{1}{2} \dot{V}_{fw} \Pi_{sw} = \frac{\hat{\alpha}}{4} \Pi_{sw}^2$. Note that this value ignores irreversible effects and reduces osmotic force through dilution [38].

The maximum work that could be obtained from the same amount of freshwater and an arbitrary amount of saltwater at Π_{sw} is $\dot{W}_{max} = \dot{V}_{fw} \Pi_{sw} = 2\dot{W}_{best, max}$ [29]. Hence, one can argue that in the standard PRO system half of the work potential is lost.

As discussed above, the entering saltwater is in non-equilibrium with the freshwater at the other side of the membrane, and entropy is generated within the module. The loss of work potential is proportional to the entropy generation. From eq. (15) it follows that less entropy will be generated within a module if the hydraulic pressure difference ΔP across the membrane is closer to the osmotic pressure of the entering saltwater. With this in mind, we shall now consider multistage PRO systems where a series of membrane modules operate at lower and lower hydraulic pressures, which can be adjusted such that entropy generation is reduced, and more work is generated.

For our consideration of *n*-stage systems we only employ pumps and turbines, in an effort to show how optimization of intermediate hydraulic pressures yields increased power generation. The question how pressure exchangers can be incorporated into two-stage settings will be considered in the second part of the paper.

3.2 Model for *n*-stage system

We model a PRO system that has one pump, *n* membrane modules, and *n* turbines as depicted in Figure 4. Saltwater with osmotic pressure Π_{sw} is pressurized by the pump (*P*) from environmental pressure P_0 to the inlet pressure P_1 , and enters the first membrane module (MM_1) with volumetric flow \dot{V}_{sw} . On the other side of the membrane freshwater is introduced at environmental pressure, and some of it is drawn across the membrane. Hence, a stream of brackish water at osmotic pressure Π_2 leaves MM_1 at the same pressure, P_1 , since we ignore hydraulic pressure losses everywhere in the system. Using the first turbine (T_1) the hydraulic pressure is now dropped to P_2 , and work is extracted. In the ensuing membrane module–turbine

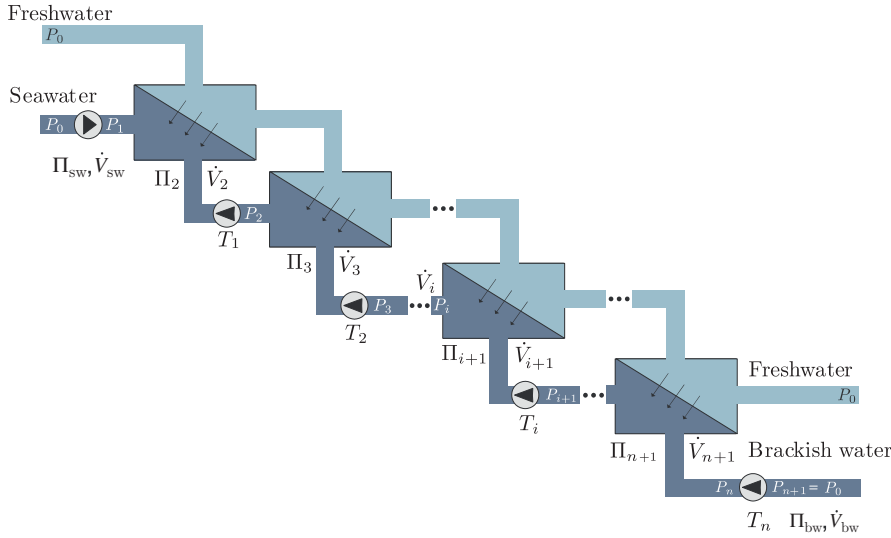


Figure 4: PRO system with a single pump and n stages consisting of membrane module and turbine. For stage i , hydraulic and osmotic pressures, and volume flow, at the module inlet are P_i , Π_i , and \dot{V}_i , and their respective values at the turbine exit are P_{i+1} , Π_{i+1} , \dot{V}_{i+1} . The freshwater entering all modules is at P_0 .

pairs ($MM_i - T_i$), more freshwater is drawn in, while the hydraulic pressure is further lowered (P_{i+1}), and work is produced in the turbines. After the last turbine (T_n) the pressure is back to P_0 .

Each segment i of this chain of membrane-turbine pairs is described by the hydraulic pressures P_i , P_{i+1} , and the osmotic pressures Π_i , Π_{i+1} at inlet and exit, and the incoming and exiting volume flows \dot{V}_i , \dot{V}_{i+1} . For the first module, we have $\Pi_1 = \Pi_{sw}$, $\dot{V}_1 = \dot{V}_{sw}$, and for the last module we have $P_{n+1} = P_0$.

The net work for the n -stage PRO system as in Figure 4 is with eqs. (4) and (5):

$$\begin{aligned} \dot{W}_{\text{net}} &= \dot{W}_P + \dot{W}_{T_1} + \dot{W}_{T_2} + \dots + \dot{W}_{T_n} \\ &= \frac{1}{\eta_p} (P_0 - P_1) \dot{V}_1 + \sum_{i=1}^n [\eta_T (P_i - P_{i+1}) \dot{V}_{i+1}]. \end{aligned} \quad (16)$$

Using eqs. (3) and (12), the volumetric flow of the salt solution leaving membrane module MM_i after drawing water and its osmotic pressures are

$$\dot{V}_{i+1} = \dot{V}_1 \frac{\Pi_1}{\Pi_{i+1}}, \quad (17)$$

$$\Pi_{i+1} = \Pi_i (1 - \eta_{MM}) + (P_i - P_0) \eta_{MM}. \quad (18)$$

For set values of turbine, pump, and membrane efficiencies, the net power output \dot{W}_{net} of the system depends on the intermediate hydraulic pressures P_i , $i = 1, \dots, n$, which appear in eq. (16) explicitly as well as implicitly through eqs. (17) and (18). These pressures must be chosen to optimize system performance, which immediately leads to the question how optimum performance is to be defined.

3.3 Target functions for optimization

In the literature on PRO systems, it is common to consider the power density of the membrane, i. e. the amount of power produced per unit area as the measure of system quality [1, 6, 8, 10]. This assumes that the main cost for building and operating the system is the membrane, while the salt- and freshwater flows are considered to be freely available.

In our framework, which is based on module and device efficiencies, the concept of power density (power per membrane area) is not accessible. Consideration of membrane area is only possible with a detailed flow model that resolves the flows through the membrane modules. Such a detailed membrane model can be included into the analysis of multistage PRO; this will be discussed elsewhere.

In the following, we focus on the work per flow volume as the parameter to optimize, where we distinguish between three different flows for the definition:

In areas where freshwater is scarce, one should optimize for freshwater use, so that one must optimize the work per litre of total freshwater drawn:

$$w_{fw} = \frac{\dot{W}_{net}}{\dot{V}_{n+1} - \dot{V}_0} = \frac{\dot{W}_{net}}{\dot{V}_{fw}}. \quad (19)$$

Similarly, in areas where the incoming saltwater must be heavily pre-treated, one should optimize for best use of saltwater flow, that is optimize the work per litre of saltwater fed:

$$w_{sw} = \frac{\dot{W}_{net}}{\dot{V}_1} = \frac{\dot{W}_{net}}{\dot{V}_{sw}}. \quad (20)$$

Finally, we consider optimization of the work per litre of exit stream:

$$w_{exit} = \frac{\dot{W}_{net}}{\dot{V}_{n+1}} = \frac{\dot{W}_{net}}{\dot{V}_{sw} + \dot{V}_{fw}},$$

which is related to the overall size of the PRO system.

In the above definitions, \dot{V}_{sw} is the volume flow of salt water entering the system, and \dot{V}_{fw} is the total amount of freshwater drawn across the membranes. To obtain insight into the performance of the multistage systems, we consider the maximum extractable work, which is determined in Appendix, eq. (36) with $P = P_{fw} = P_0$, $\dot{S}_{gen} = 0$, see also Ref. [12]:

$$\dot{W}_{rev} = \Pi_{sw} \dot{V}_{sw} \ln \left(1 + \frac{\dot{V}_{fw}}{\dot{V}_{sw}} \right). \quad (21)$$

The optimizations below yield different volumetric flow ratios $\dot{V}_{fw}/\dot{V}_{sw}$ for the systems considered and therefore the maximum extractable work differs. The effectiveness of a particular configuration as optimized is represented by the fraction of the work produced to the maximum available in terms of the stream that is the focus of the optimization, as discussed above. In particular we have

$$\begin{aligned} w_{exit}^{rev} &= \frac{\dot{W}_{rev}}{\dot{V}_{sw} + \dot{V}_{fw}} = \Pi_{sw} \frac{\ln \left(1 + \frac{\dot{V}_{fw}}{\dot{V}_{sw}} \right)}{1 + \frac{\dot{V}_{fw}}{\dot{V}_{sw}}}, \\ w_{fw}^{rev} &= \frac{\dot{W}_{rev}}{\dot{V}_{fw}} = \Pi_{sw} \frac{\dot{V}_{sw}}{\dot{V}_{fw}} \ln \left(1 + \frac{\dot{V}_{fw}}{\dot{V}_{sw}} \right), \\ w_{sw}^{rev} &= \frac{\dot{W}_{rev}}{\dot{V}_{sw}} = \Pi_{sw} \ln \left(1 + \frac{\dot{V}_{fw}}{\dot{V}_{sw}} \right). \end{aligned} \quad (22)$$

Note that w_{exit}^{rev} has a maximum for $\frac{\dot{V}_{fw}}{\dot{V}_{sw}} = \exp[1] - 1 = 1.7183$, while w_{fw}^{rev} and w_{sw}^{rev} have boundary maxima for $\frac{\dot{V}_{fw}}{\dot{V}_{sw}} \rightarrow 0$ and $\frac{\dot{V}_{fw}}{\dot{V}_{sw}} \rightarrow \infty$, respectively. The respective maximum values are $\{w_{exit}^{rev}, w_{fw}^{rev}, w_{sw}^{rev}\}_{max} = \{\Pi_{sw}/\exp[1], \Pi_{sw}, \infty\}$.

3.4 Results

We now present optimization results for PRO systems of up to 20 stages. For all systems, we have set turbine and pump efficiencies to $\eta_T = \eta_P = 0.9$ and considered membrane effectiveness $\eta_{MM} = 0.65, 0.85$,

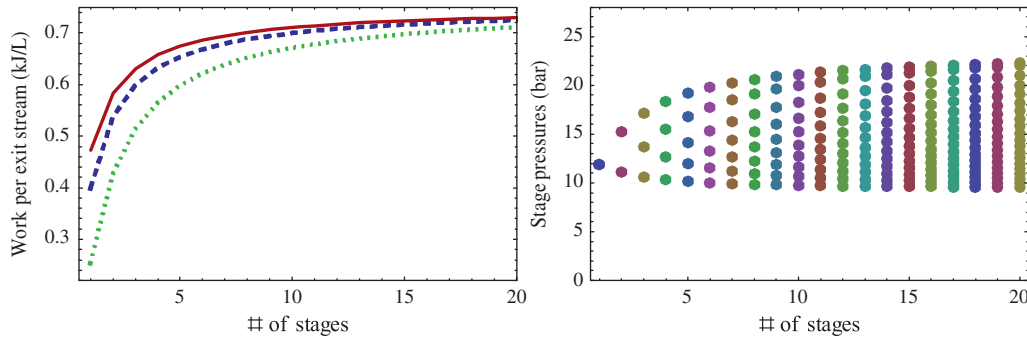


Figure 5: Left: Optimized work per exit stream (kJ/L) over number of stages for $\eta_P = \eta_T = 0, 9$, and $\eta_{MM} = 0.95$ (red, continuous line), $\eta_{MM} = 0.85$ (blue, dashed) and $\eta_{MM} = 0.65$ (green, dotted). Right: Intermediate pressures over number of stages for the case with $\eta_{MM} = 0.85$.

0.95. The incoming saltwater is seawater with osmotic pressure $\Pi_{sw} = \Pi_0 = 28$ bar. Figures 5–7 show the relative work (w_{exit} , w_{fw} , or w_{sw}) over the number of stages, as well as the hydraulic pressures P_i for the cases with $\eta_{MM} = 0.85$.

Optimization is done by means of a Mathematica code that evaluates the condition for optimum work, $\frac{\partial w}{\partial P_i} = 0$ ($i = 1, 2, \dots, n$) for $w = \{w_{exit}, w_{fw}, w_{sw}\}$, to find the intermediate pressures P_i for optimum performance.

3.4.1 Work per exit stream

We first consider the work per exit stream. Figure 5 shows the optimized work $w_{exit} = \frac{\dot{W}_{net}}{V_{n+1}}$ over the number of stages for membrane module effectiveness $\eta_{MM} = 0.65, 0.85, 0.95$, and the optimal intermediate pressures for the case with $\eta_{MM} = 0.85$. For all membrane modules, increase of the number of stages leads to an increase in work; for larger number of stages the curves converge towards a maximum of ~ 0.72 kJ/L. The optimum pressures P_i lie in a finite interval, for the case depicted $P_{max} \simeq 22.3$ bar and $P_{min} \simeq 9.5$ bar. The maximum for work and the range of pressure depend on the turbine and pump efficiencies; as the efficiencies increase, the inlet pressure ($P_1 = P_{max}$) approaches the osmotic pressure of the incoming saltwater.

We also compared the results to the reversible work w_{exit}^{rev} defined in eq. (22) and found that with more stages, the work produced is closer to the reversible work. For the case with $\eta_{MM} = 0.85$, the single-stage system delivers only 40% of w_{exit}^{rev} , the two-stage system delivers 52% of w_{exit}^{rev} , while the 20-stage system delivers 72% of w_{exit}^{rev} . Moreover, for perfect pumps, turbines and modules ($\eta_P = \eta_T = \eta_{MM} = 1$), the system work increases from 72% of w_{exit}^{rev} for a single-stage system to 99% of w_{exit}^{rev} for 25 stages. The better performance of multistage systems is a direct reflection of smaller entropy generation (15) in the modules, hence, better conversion of the available energy.

3.4.2 Work per freshwater stream

Figure 6 shows the result of the optimization for best use of freshwater, so that $w_{fw} = \frac{\dot{W}_{net}}{V_{fw}}$ becomes maximal. The result shares the main characteristics with the previous case, only that the pressure band is narrower, and the final exiting pressure is higher. Again, as more stages are added, the maximum work for the three membrane modules converges. In comparison to the optimization for exit flow (i. e. system size), the volume ratio between incoming saltwater and total freshwater drawn is larger, which implies larger system size. With increasing turbine, pump, and module efficiencies, the pressure band becomes rather narrow

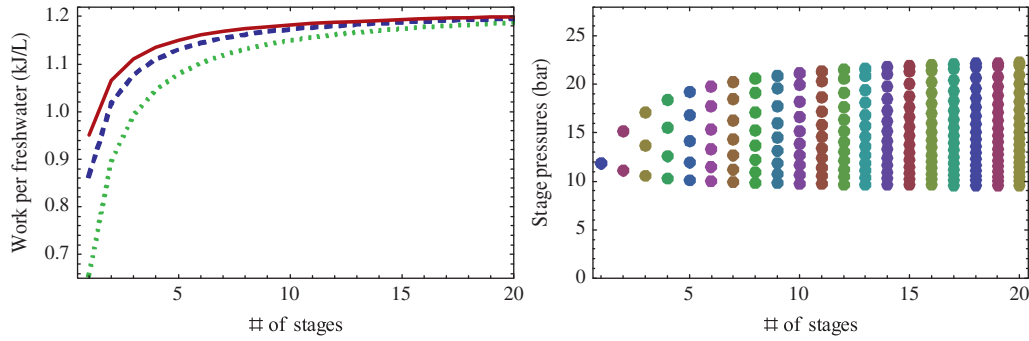


Figure 6: Left: Optimized work per freshwater drawn in kJ/L over number of stages for $\eta_P = \eta_T = 0.9$, and $\eta_{MM} = 0.95$ (red, continuous line), $\eta_{MM} = 0.85$ (blue, dashed) and $\eta_{MM} = 0.65$ (green, dotted). Right: Intermediate pressures over number of stages for the case with $\eta_{MM} = 0.85$.

with values close to the osmotic pressure of the incoming saltwater, and the work produced approaches the value $\dot{W} = \Pi_{sw} \dot{V}_{fw}$ [29]. This is a theoretical optimum, which corresponds to an infinite ratio between saltwater and freshwater flows ($\dot{V}_{sw}/\dot{V}_{fw} \rightarrow \infty$ or $\dot{V}_{fw}/\dot{V}_{sw} \rightarrow 0$) as discussed already in Section 3.3.

3.4.3 Work per saltwater stream

Finally, we consider the optimization of work per saltwater flow, $w_{sw} = \frac{\dot{W}_{net}}{\dot{V}_{sw}}$, with results depicted in Figure 7. Again, we see a band of pressures, where now the maximum pressure is relatively low. Work curves for different membrane modules do not converge – more effective modules draw more freshwater and give increased power generation. As efficiencies of membrane, pump, and turbines increase, the maximum pressure approaches the environmental pressure P_0 , and the freshwater flow and power output become larger and larger. Indeed, for the fully reversible case (see Section 3.3), the work that can be obtained per litre of saltwater approaches infinity – this requires infinite volume flow of freshwater, $\dot{V}_{fw}/\dot{V}_{sw} \rightarrow \infty$ [29].

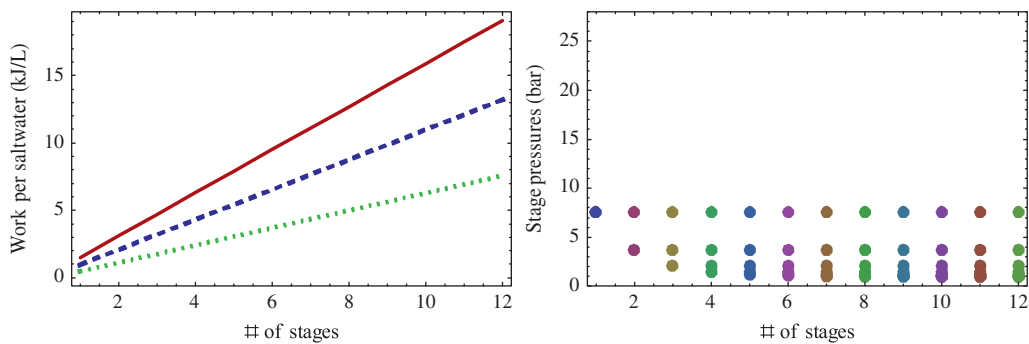


Figure 7: Left: Optimized work per incoming saltwater (kJ/L) over number of stages for $\eta_P = \eta_T = 0.9$, and $\eta_{MM} = 0.95$ (red, continuous line), $\eta_{MM} = 0.85$ (blue, dashed) and $\eta_{MM} = 0.65$ (green, dotted). Right: Intermediate pressures over number of stages for the case with $\eta_{MM} = 0.85$.

3.5 Summary

As the above discussion shows, the optimal work that can be obtained in osmotic power plants and the optimal intermediate pressures in a multistage system depend on the choice of the target function for optimization. When maximizing the work per freshwater intake, or the work per saltwater intake, we find

pressure and flow conditions that in the limit of reversible device performance lead to infinite flows, hence would require infinitely large systems. From this observation, one probably will be inclined to consider the work per exit stream as the best target function. Nevertheless, for optimized irreversible systems all flows remain finite, and different target functions (w_{exit} , w_{fw} , w_{sw}) lead to quite different choices for intermediate pressures.

Our results indicate that multistage PRO systems will have better performance than single-stage systems. While the additional stages increase performance, they lead to more complicated and larger systems, which are more costly to build and maintain. It will depend on costs for building, maintenance, and operation what configuration would make the best economical sense. Certainly one will avoid a large number of stages, but it might be worthwhile to consider two- or three-stage PRO systems as alternatives. For the above discussion we considered pumps and turbines only, in order to highlight the general advantage of multistage systems. In general, pumps and turbines have insufficient efficiencies, which is the reason why single-stage PRO systems are always considered with pressure exchangers. In the next section, we consider the use of pressure exchangers in one- and two-stage PRO systems.

4 Single-stage and two-stage PRO configurations

The detailed discussion of multistage PRO systems in the previous section indicates that multistaging will improve power generation. For simple access to systems with an arbitrary number of stages we only used pumps and turbines, which are, under most conditions, less efficient than pressure exchangers. The natural next step, therefore, is to incorporate pressure exchangers into multistage systems. In the following, we discuss one- and two-stage systems only, which employ pressure exchangers, and additional pumps and turbines. Specifically, we compare four different configurations: (1PT) single-stage system with pump and turbine, (1PX) single-stage system with pressure exchanger, (2PT) two-stage system with pump and turbines, (2PX) two-stage system with two pressure exchangers. Systems 1PT and 2PT are special cases of the multistage systems discussed above, and system 1PX is the standard single-stage PRO system. The single-stage configurations are rather similar, 1PT results from 1PX, when the pressure exchanger is replaced by a pump–turbine pair.

The main reason to consider only two-stage systems is the difficulty to fit pressure exchangers into systems with three or more stages; also, the above results show that the relative incremental increase of adding stages becomes smaller and smaller with increasing number of stages.

In the following sections, the configurations 1PX and 2PX are described, and their power generation in dependence of intermediate hydrostatic pressures is determined. After that, the modelled performance of the four configurations is compared, for different optimization scenarios (w_{exit} , w_{fw} , w_{sw}).

4.1 1PX: Single-stage PRO with pressure exchanger

As a benchmark system we consider the standard single-stage PRO system model, as depicted already in Figure 1. Since the pressure exchanger experiences pressure loss δP , a feed pump is required to pressurize the incoming saltwater flow \dot{V}_{sw} to the pressure exchanger inlet pressure $P_0 + \delta P$. Then, the saltwater is pressurized to $P_1 - \delta P$ in the pressure exchanger and further to P_1 in a booster pump. The pressurized saltwater enters the membrane module, where it draws the total freshwater flow \dot{V}_{fw} across the membrane; pressure loss in the module is ignored. After the membrane the resulting brackish water flow is split with one part (\dot{V}_{sw}) going towards the pressure exchanger, and the remainder (\dot{V}_{fw}) entering the turbine to generate power, with the turbine exit flow at P_0 . This configuration is similar to the one proposed by Loeb et al. and later adopted in the first PRO power plant in Norway [8, 14].

The net work of the system is the sum of turbine and pump contributions, with $\Delta P = P_1 - P_0$,

$$\dot{W}_{\text{net}} = \eta_T \dot{V}_{\text{fw}} \Delta P - \frac{2}{\eta_P} \dot{V}_{\text{sw}} \delta P, \quad (23)$$

where the freshwater inflow is determined from eq. (3):

$$\dot{V}_{\text{fw}} = \dot{V}_{\text{sw}} \left(\frac{\Pi_{\text{sw}}}{\Pi_{\text{bw}}} - 1 \right) = \dot{V}_{\text{sw}} \frac{\Pi_{\text{sw}} - \Delta P}{\left(\frac{1}{\eta_{\text{MM}}} - 1 \right) \Pi_{\text{sw}} + \Delta P}. \quad (24)$$

4.2 2PX: Two-stage PRO with pressure exchangers

A possible configuration for two-stage PRO with pressure exchangers is depicted in Figure 8. The incoming saltwater flow \dot{V}_{sw} is delivered to the first pressure exchanger by a feed pump (PF) at pressure $P_0 + \delta P$, and leaves the first pressure exchanger at pressure $P_2 - \delta P$. The saltwater flow enters the second pressure exchanger, where the pressure is further increased to $P_1 - \delta P$ and is then delivered by the first booster pump (PB1) to the first membrane unit, at pressure P_1 . The first membrane module draws the volume flow $\dot{V}_{\text{fw},1}$ of freshwater. After the module, the resulting brackish water flow is divided into the streams of flow rate \dot{V}_{sw} and $\dot{V}_{\text{fw},1}$. The stream at rate \dot{V}_{sw} is depressurized in the second pressure exchanger to $P_2 - 2\delta P$ (recall that the low-pressure stream entering the pressure exchanger is at $P_2 - \delta P$), and then pressurized by another booster pump (PB2) to the inlet pressure of the second membrane module, P_2 . The remaining flow, at rate \dot{V}_{fw} and pressure P_1 , drives the first turbine (T1), which it leaves at P_2 . Now both streams of brackish water are combined and enter the second membrane module, which draws more freshwater in, at rate $\dot{V}_{\text{fw},2}$. After the module, the stream of further diluted brackish water, at P_2 , is split again, with the flow \dot{V}_{sw} going to the first pressure exchanger, and the remaining flow at rate $(\dot{V}_{\text{fw},1} + \dot{V}_{\text{fw},2})$ entering the second turbine, which they leave at pressure P_0 .

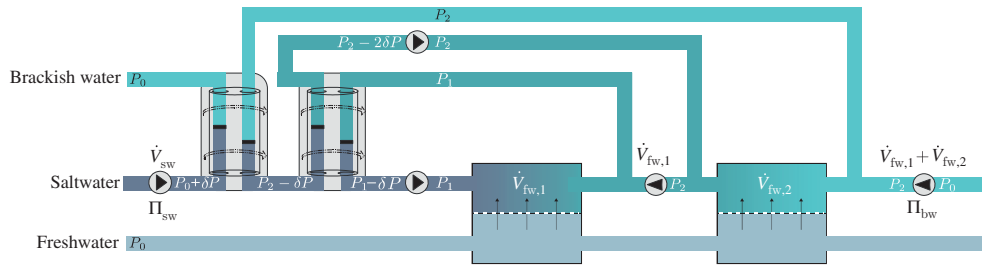


Figure 8: 2PX: Two-stage PRO system with two pressure exchangers. A feed pump and two booster pumps are required to compensate for the pressure loss in the pressure exchangers. Two turbines generate power and lower the hydraulic pressure.

This configuration employs three pumps, the feed pump (PF) and two booster pumps (PB), which have the work requirements

$$\dot{W}_{\text{PF}} = -\frac{1}{\eta_P} \dot{V}_{\text{sw}} \delta P, \quad \dot{W}_{\text{PB1}} = -\frac{1}{\eta_P} \dot{V}_{\text{sw}} \delta P, \quad \dot{W}_{\text{PB2}} = -\frac{2}{\eta_P} \dot{V}_{\text{sw}} \delta P, \quad (25)$$

while the two turbines deliver the power

$$\dot{W}_{T1} = \eta_T \dot{V}_{\text{fw},1} (P_1 - P_2), \quad \dot{W}_{T2} = \eta_T (\dot{V}_{\text{fw},1} + \dot{V}_{\text{fw},2}) (P_2 - P_0). \quad (26)$$

The net work is the sum over all contributions from pumps and turbines:

$$\dot{W}_{\text{net}} = \eta_T \dot{V}_{\text{fw},1} (P_1 - P_0) + \eta_T \dot{V}_{\text{fw},2} (P_2 - P_0) - \frac{4}{\eta_P} \dot{V}_{\text{sw}} \delta P. \quad (27)$$

The volume flows drawn into the modules are, from eq. (13),

$$\dot{V}_{fw,1} = \dot{V}_{sw} \left(\frac{\Pi_{sw}}{\Pi_1} - 1 \right), \quad \dot{V}_{fw,2} = (\dot{V}_{fw,1} + \dot{V}_{sw}) \left(\frac{\Pi_1}{\Pi_2} - 1 \right), \quad (28)$$

where $\Pi_{1,2}$ are the osmotic pressures at the membrane module exits; these follow from eq. (12) as

$$\Pi_1 = (1 - \eta_{MM})\Pi_{sw} + \eta_{MM}(P_1 - P_0), \quad (29)$$

$$\Pi_2 = (1 - \eta_{MM})\Pi_1 + \eta_{MM}(P_2 - P_0). \quad (30)$$

Combining the above relations gives an explicit expression for the power generation \dot{W}_{net} , as a function of the intermediate pressures P_1 and P_2 , and the entering saltwater flow \dot{V}_{sw} , with parameters η_{MM} , η_P , η_T and δP . For given parameters, the intermediate pressures can, again, be found by optimization.

4.3 Analysis of PRO configurations

We proceed with the comparison of the four systems at hand, which are: (1PT, 2PT) single-stage and two-stage systems with pumps and turbines, (1PX, 2PX) single-stage and two-stage systems with pressure exchangers, pumps, and turbines. For comparison, we consider again the case of saltwater with osmotic pressure $\Pi_{sw} = 28$ bar, freshwater at $P_0 = 1$ bar, turbine and pump efficiencies $\eta_T = \eta_P = 0.9$, and pressure exchanger loss $\delta P = 0.5$ bar, and membrane module effectiveness $\eta_{MM} = 0.95, 0.85, 0.65$. With these parameters fixed, the performance of all systems depends on the intermediate hydraulic pressures (P_1 for single stage, or P_1, P_2 for two stage), which are obtained from optimization. As before, we consider different optimization scenarios, based on overall system size (optimized $w_{exit} = \dot{W}_{net} / (\dot{V}_{sw} + \dot{V}_{fw})$), use of freshwater (optimized $w_{fw} = \dot{W}_{net} / \dot{V}_{fw}$), or use of saltwater (optimized $w_{sw} = \dot{W}_{net} / \dot{V}_{sw}$). The results for the three optimization cases are presented next.

4.3.1 Work per exit stream w_{exit}

Before we compare single-stage and two-stage systems, we use our models to determine the optimum hydraulic pressure difference $\Delta P = P_1 - P_0$ for the single-stage PRO systems 1PX and 1PT, which yields for the system with pressure exchanger

$$\Delta P_{max, 1PX} = \frac{\Pi_{sw}}{2} - \frac{\delta P}{\eta_T \eta_P},$$

and for the system with pumps and turbines

$$\Delta P_{max, 1PT} = \frac{\Pi_{sw}}{2} - \frac{1 - \eta_P \eta_T}{2\eta_{MM}} \Pi_{sw}.$$

For fully reversible pumps, turbines and pressure exchangers ($\eta_T = \eta_P = 1, \delta P = 0$), the optimal hydraulic pressure difference is half the osmotic pressure, while a smaller pressure is required when the systems are irreversible. Interestingly, the optimum pressure for the system with pressure exchanger (1PX) is independent of the membrane module efficiency, while for the 1PT system the pressure reduction depends on it.

Now we proceed with the comparison of all four systems, for which the optimized data are laid out in Table 1. For each of the four systems, the table gives the optimized work w_{exit} , the corresponding hydraulic pressures P_i , and the freshwater to saltwater ratios $\dot{V}_{fw} / \dot{V}_{sw}$. Moreover, we give the ratio between the optimized work and the maximum work that could be obtained from reversible mixing of the streams, w_{exit}^{rev} , as defined in eq. (22).

We focus on the data for work, where we see that for all three values of membrane module effectiveness ($\eta_{MM} = 0.95, 0.85, 0.65$) the single-stage systems 1PT and 1PX produce less work than the two-stage systems

Table 1: Optimization results for work per exit stream, with membrane effectiveness $\eta_{MM} = 0.95, 0.85, 0.65$.

| | Single-stage PRO | | Two-stage PRO | | |
|--------------------|------------------|--------|---------------|--------------|--|
| | 1PT | 1PX | 2PT | 2PX | |
| $\eta_{MM} = 0.95$ | 0.473 | 0.541 | 0.584 | 0.630 | w_{exit} (kJ/L) |
| | 12.20 | 14.38 | 15.86, 11.10 | 18.57, 12.36 | P_i (bar) |
| | 1.326 | 0.984 | 1.70 | 1.39 | $\dot{V}_{\text{fw}}/\dot{V}_{\text{sw}}$ |
| | 46.5 % | 56.0 % | 56.7 % | 61.7 % | $w_{\text{exit}}/w_{\text{exit}}^{\text{rev}}$ |
| $\eta_{MM} = 0.85$ | 0.399 | 0.473 | 0.538 | 0.582 | w_{exit} (kJ/L) |
| | 11.87 | 14.38 | 15.20, 11.14 | 18.02, 12.35 | P_i (bar) |
| | 1.08 | 0.798 | 1.53 | 1.25 | $\dot{V}_{\text{fw}}/\dot{V}_{\text{sw}}$ |
| | 40.4 % | 51.7 % | 52.3 % | 57.7 % | $w_{\text{exit}}/w_{\text{exit}}^{\text{rev}}$ |
| $\eta_{MM} = 0.65$ | 0.253 | 0.335 | 0.427 | 0.463 | w_{exit} (kJ/L) |
| | 10.91 | 14.38 | 13.40, 11.25 | 16.87, 12.41 | P_i (bar) |
| | 0.724 | 0.514 | 1.17 | 0.937 | $\dot{V}_{\text{fw}}/\dot{V}_{\text{sw}}$ |
| | 28.6 % | 43.7 % | 42.7 % | 48.5 % | $w_{\text{exit}}/w_{\text{exit}}^{\text{rev}}$ |

2PT and 2PX, and the pump–turbine systems produce less work than the systems with pressure exchangers. It is worthwhile to note that, for the given range of parameters, the two-stage pump–turbine system 2PT produces more work than the single-stage system with pressure exchanger 1PX. These results confirm the possible advantages of multistage PRO systems.

We also note that the work w_{exit} for all systems lies well below the reversible work $w_{\text{exit}}^{\text{rev}}$ (best case is 61.7 %). This is due partly to the irreversibilities in the systems (pump/turbines/membrane/PX), but also due to the limitations of the chosen design. Even if all elements work at their best ($\eta_T = \eta_P = \eta_{MM} = 1$, $\gamma_{\text{PX}} = 0$) the single-stage systems reach only 72.1% of $w_{\text{exit}}^{\text{rev}}$, while the two-stage systems reach 82.2% of $w_{\text{exit}}^{\text{rev}}$. The reason for the loss is entropy generation in the membrane modules, which operate at finite pressure differences $\Pi - \Delta P$, see eq. (15).

4.3.2 Work per freshwater stream w_{fw}

Table 2 shows the optimized results for the work per freshwater stream, w_{fw} . The behaviour now is quite different. For all three values of the membrane efficiency, the single-stage system with pressure exchanger (1PX) produces most work per volume of freshwater, and both systems with pressure exchanger (1PX, 2PX)

Table 2: Optimization results for work per freshwater stream, with membrane effectiveness $\eta_{MM} = 0.95, 0.85, 0.65$.

| | Single-stage PRO | | Two-stage PRO | | |
|--------------------|------------------|--------|---------------|--------------|--|
| | 1PT | 1PX | 2PT | 2PX | |
| $\eta_{MM} = 0.95$ | 0.951 | 1.56 | 1.07 | 1.39 | w_{fw} (kJ/L) |
| | 16.48 | 22.97 | 19.14, 15.87 | 23.87, 19.89 | P_i (bar) |
| | 0.739 | 0.257 | 0.860 | 0.466 | $\dot{V}_{\text{fw}}/\dot{V}_{\text{sw}}$ |
| | 45.3 % | 62.0 % | 52.7 % | 60.3 % | $w_{\text{fw}}/w_{\text{fw}}^{\text{rev}}$ |
| $\eta_{MM} = 0.85$ | 0.865 | 1.48 | 1.02 | 1.34 | w_{fw} (kJ/L) |
| | 15.76 | 22.62 | 18.53, 15.79 | 23.46, 19.68 | P_i (bar) |
| | 0.672 | 0.240 | 0.814 | 0.445 | $\dot{V}_{\text{fw}}/\dot{V}_{\text{sw}}$ |
| | 40.4 % | 59.1 % | 49.7 % | 57.7 % | $w_{\text{fw}}/w_{\text{fw}}^{\text{rev}}$ |
| $\eta_{MM} = 0.65$ | 0.656 | 1.32 | 0.896 | 1.20 | w_{fw} (kJ/L) |
| | 13.86 | 21.71 | 16.74, 15.49 | 22.39, 19.11 | P_i (bar) |
| | 0.542 | 0.204 | 0.704 | 0.395 | $\dot{V}_{\text{fw}}/\dot{V}_{\text{sw}}$ |
| | 29.3 % | 51.7 % | 42.3 % | 51.0 % | $w_{\text{fw}}/w_{\text{fw}}^{\text{rev}}$ |

produce more work than the pump–turbine systems (1PT, 2PT). We note that the intermediate pressures are higher than in the previous case (w_{exit}), which means that pumps and turbines operate at higher pressure differences. Since turbine and pump losses are proportional to the pressure differences, higher operating pressures increase the losses. The two intermediate pressures for system 2PX are close to each other, so that the loss factor for the second pressure exchanger is rather large; specifically, we have $\gamma_{\text{PX}} = \frac{2\delta P}{P_1 - P_2} \simeq 0.5$. This leads to a comparatively large loss for system 2PX, and the advantage for system 1PX.

The results also show that system 1PX gives the best output relative to the reversible work $w_{\text{fw}}^{\text{rev}}$.

4.3.3 Work per saltwater stream w_{sw}

Table 3 shows the optimized results for the work per saltwater stream, w_{sw} . Again, the behaviour is quite different. Since the intermediate hydraulic pressures are relatively low, the overall loss in pumps and turbines, which is proportional to pressure differences, is relatively small, which renders the pump–turbine systems competitive to the pressure exchanger systems, for which the losses are proportional to the fixed value δP . For the data used, the two-stage pump–turbine system yields more work than the corresponding two-stage system with pressure exchanger. The single-stage systems 1PT and 1PX produce comparable work at high membrane module efficiency, with small advantages of 1PX over 1PT as membrane efficiency becomes smaller. Finally, the two-stage systems produce about twice the power of single-stage systems, but require considerably larger freshwater flows. All systems harvest only about one-third of the reversible work available from the streams \dot{V}_{sw} , \dot{V}_{fw} .

Table 3: Optimization results for work per saltwater stream, with membrane effectiveness $\eta_{\text{MM}} = 0.95, 0.85, 0.65$.

| | Single-stage PRO | | Two-stage PRO | | |
|---------------------------|------------------|--------|---------------|-------------|--|
| | 1PT | 1PX | 2PT | 2PX | |
| $\eta_{\text{MM}} = 0.95$ | 1.50 | 1.49 | 3.10 | 2.98 | w_{sw} (kJ/L) |
| | 5.46 | 6.12 | 5.46, 2.03 | 6.12, 2.14 | P_i (bar) |
| | 3.97 | 3.47 | 21.2 | 19.0 | $\dot{V}_{\text{fw}}/\dot{V}_{\text{sw}}$ |
| | 33.4 % | 35.5 % | 35.7 % | 35.5 % | $w_{\text{sw}}/w_{\text{sw}}^{\text{rev}}$ |
| $\eta_{\text{MM}} = 0.85$ | 0.962 | 1.00 | 2.08 | 2.00 | w_{sw} (kJ/L) |
| | 7.54 | 8.82 | 7.54, 3.72 | 8.82, 4.03 | P_i (bar) |
| | 1.87 | 1.58 | 6.41 | 5.67 | $\dot{V}_{\text{fw}}/\dot{V}_{\text{sw}}$ |
| | 32.6 % | 37.7 % | 37.0 % | 37.7 % | $w_{\text{sw}}/w_{\text{sw}}^{\text{rev}}$ |
| $\eta_{\text{MM}} = 0.65$ | 0.455 | 0.535 | 1.10 | 1.07 | w_{sw} (kJ/L) |
| | 8.86 | 11.41 | 8.86, 6.54 | 11.41, 7.16 | P_i (bar) |
| | 0.878 | 0.690 | 2.17 | 1.86 | $\dot{V}_{\text{fw}}/\dot{V}_{\text{sw}}$ |
| | 25.8 % | 36.4 % | 34.1 % | 36.4 % | $w_{\text{sw}}/w_{\text{sw}}^{\text{rev}}$ |

5 Conclusions

We have examined multistage systems for PRO, built by combinations of pumps (P), turbines (T), pressure exchangers (PX), and membrane modules (MM). The performance of all elements are described by standard thermodynamic efficiency measures, and the overall system performance was optimized for different target functions, namely the work per exit stream, the work per freshwater drawn, and the work per saltwater drawn. The optimization yields the intermediate pressures for the stages, which differ widely between the different optimization targets.

Specifically, we considered pump–turbine–membrane systems with up to 20 stages, where for all scenarios addition of stages improves the performance. Here, the biggest relative improvement occurs at lower stage numbers, i. e. when going from single-stage to two- or three-stage systems, while for systems with large number of stages the addition of more stages leads to relatively small improvements.

Since, for large pressure differences, pump–turbine pairs compare unfavourably to pressure exchangers, we considered single- and two-stage systems with PT pairs or PX– P – T combinations, again comparing optimum power generation for the three target functions.

The main findings can be summarized as follows:

- Pressure exchangers exhibit pressure loss δP independent of the pressure ratio $P_H - P_L$. Hence, their loss factors $\gamma = \frac{2\delta P}{P_H - P_L}$ is small when the pressure difference is large, but the loss factor will be large for small pressure differences. Accordingly, for small pressure difference $P_H - P_L$, pressure exchangers will be less efficient than pump–turbine pairs.
- Multistage systems generally have better performance. Exceptions are systems with pressure exchangers and small pressure differences across the pressure exchanger, where the PX loss becomes relatively large.
- All results depend markedly on the efficiency measures for P , T , PX, and MM. The typical efficiency measures for P , T , and PX utilized in the model are attained with current technology.
- Different target functions for optimization (based on work per exit flow, saltwater inflow, or freshwater inflow, w_{exit} , w_{fw} , w_{sw}) yield rather different optimum conditions, for operation of single-stage and multistage systems. In particular, the intermediate pressures depend strongly on the choice of the target function. In general, the saltwater inflow and freshwater inflow target functions lead to relatively less effective systems than the target of work per exit flow; the intermediate pressures are higher and the fraction of the resource that is harvested is lower at a given module efficiency.
- Although highly efficient membrane modules are desirable, the advantage of a second stage in PRO, either 2PT relative to 1PT or 2PX relative to 1PX, persists over all module efficiencies based on work per exit stream. Significant system efficiency improvements are accessible through the use of two-stage PRO designs even with relatively inefficient modules.

Our analysis is based on an idealized seawater–freshwater pair. We agree that this resource – vast as it is on the planetary scale – may be insufficiently energetic locally to offset pre-treatment energy costs such that other PRO implementations offer better prospects [11]. Hybrid RO desalination–PRO systems in which PRO energy generation partially reduces the energy required for desalination is one appealing alternative. The type of system thermodynamic analysis we have done here is directly applicable to exploring the complex designs such systems require, including additional target functions such as the work per unit freshwater produced.

Deeper insight into multistage PRO systems requires detailed modelling of membrane units, with accurate description of flow patterns, concentration polarization, hydraulic losses, salt permeation, and other causes for irreversible losses. We expect that counterflow designs will offer advantages in reducing membrane area, but the module efficiency definition that we have used here ensures that the inherent advantage of two-stage PRO will be preserved. Most importantly, such a model will allow to optimize the systems for membrane use, by considering the power density of the membrane as target function. The model will also be useful in defining target membrane properties as a threshold for economic construction and operation.

Acknowledgments: The authors thank Dr Peter Wild (University of Victoria) and Roghayeh Soltani (University of Victoria) for helpful discussions concerning the topics of this paper.

Funding: This research was supported by the Natural Sciences and Engineering Research Council of Canada (NSERC) grants DG 1113 (TMF) and DG 03679 (HS).

Appendix: Gibbs free energy of mixing

We consider the mixing of a flow \dot{V}_{sw} of saltwater at pressure P and mole fraction X_{sw} with a volume flow of freshwater at pressure P_{fw} ; the resulting mixture is brackish water at P , X_{bw} . Combining the first and second law of thermodynamics, we find that the sum of power produced/consumed and entropy generation is equal to the Gibbs free energy of mixing [29]:

$$\dot{W} + T\dot{S}_{gen} = -\Delta\dot{G}, \quad (31)$$

with

$$\Delta\dot{G} = \sum_{out} \dot{n}_\alpha \bar{\mu}_\alpha - \sum_{in} \dot{n}_\alpha \bar{\mu}_\alpha \quad (32)$$

Here, \dot{n}_α denotes the mole flows of the components (salt, water) entering and leaving, and $\bar{\mu}_\alpha$ are the corresponding molar chemical potentials. We assume ideal mixtures throughout, so that $\bar{\mu}_\alpha(P, T, X_\beta) = \bar{g}_\alpha(T, P) + \bar{R}T \ln X_\alpha$, where $\bar{g}_\alpha(T, P)$ is the molar Gibbs free energy of α alone.

In particular, we have for the outflow:

Brackish water

$$\begin{aligned} \text{Salt: } \bar{\mu}_s(P, T, X_{bw}) &= \bar{g}_s(P, T) + \bar{R}T \ln X_{bw}, & \dot{n}_s &= \dot{n}_{bw} X_{bw} \\ \text{Water: } \bar{\mu}_w(P, T, X_{bw}) &= \bar{g}_w(P, T) + \bar{R}T \ln(1 - X_{bw}), & \dot{n}_w &= \dot{n}_{bw}(1 - X_{bw}) \end{aligned}$$

For the inflows, we have, considering incompressible liquids,

Salt water

$$\begin{aligned} \text{Salt: } \bar{\mu}_s(P, T, X_{sw}) &= \bar{g}_s(P, T) + \bar{R}T \ln X_{sw}, & \dot{n}_s &= \dot{n}_{sw} X_{sw} \\ \text{Water: } \bar{\mu}_w(P, T, X_{sw}) &= \bar{g}_w(P, T) + \bar{R}T \ln(1 - X_{sw}), & \dot{n}_w &= \dot{n}_{sw}(1 - X_{sw}) \end{aligned}$$

Fresh water

$$\text{Water: } \bar{\mu}_w(P_{fw}, T) = \bar{g}_w(P, T) - \bar{v}_w(P - P_{fw}), \quad \dot{n}_{fw}$$

with the molar volume of water, \bar{v}_w .

The mole flows are related as

$$\dot{n}_{bw} X_{bw} = \dot{n}_{sw} X_{sw}, \quad \dot{n}_{bw} = \dot{n}_{sw} + \dot{n}_{fw} \quad (33)$$

Combining the above, we find the Gibbs free energy as

$$\begin{aligned} \Delta\dot{G} &= \dot{n}_{sw} X_{sw} \bar{R}T \ln \frac{X_{bw}}{X_{sw}} + \dot{n}_{sw}(1 - X_{sw}) \bar{R}T \ln \frac{1 - X_{bw}}{1 - X_{sw}} \\ &\quad + \dot{n}_{fw} [\bar{R}T \ln(1 - X_{bw}) + \bar{v}_w(P - P_{fw})]. \end{aligned} \quad (34)$$

Typically, the salt mole fractions X_{bw} , X_{sw} are small, and hence we can expand to first order, to find

$$\Delta\dot{G} = \dot{n}_{sw} X_{sw} \bar{R}T \ln \frac{X_{bw}}{X_{sw}} + \dot{V}_{fw}(P - P_{fw}), \quad (35)$$

where $\dot{V}_{fw} = \dot{n}_{fw} \bar{v}_w$ is the volume flow of freshwater. With $X_{bw} = \frac{\dot{n}_s}{\dot{n}_{bw}}$, $X_{sw} = \frac{\dot{n}_s}{\dot{n}_{sw}}$, and with the (slightly simplifying) assumption that mole flows are proportional to volume flows, we have $\frac{X_{bw}}{X_{sw}} = \frac{\dot{n}_{sw}}{\dot{n}_{bw}} = \frac{\dot{V}_{sw}}{\dot{V}_{sw} + \dot{V}_{fw}}$.

Finally, we replace $\dot{n}_{sw} X_{sw} = i_{sw} \dot{V}_{sw}$ to find the Gibbs free energy of mixing (salt and brackish water at P , freshwater at P_{fw}) as

$$\dot{W} + T\dot{S}_{gen} = -\Delta\dot{G} = \Pi_{sw} \dot{V}_{sw} \ln \left(1 + \frac{\dot{V}_{fw}}{\dot{V}_{sw}} \right) - \dot{V}_{fw}(P - P_{fw}); \quad (36)$$

$\Pi_{sw} = i c_{sw} \bar{R}T$ is the osmotic pressure of the saltwater. In a fully reversible process we have $\dot{S}_{gen} = 0$, while in a fully irreversible process $\dot{W} = 0$.

References

- [1] B. E. Logan and M. Elimelech, Membrane-based processes for sustainable power generation using water, *Nature* **488** (2012), no. 7411, 313–319.
- [2] R. E. Pattle, Production of electric power by mixing fresh and salt water in the hydroelectric pile, *Nature* **174** (1954), no. 4431, 660–660.
- [3] S. Loeb, Production of energy from concentrated brines by pressure-retarded osmosis: I. Preliminary technical and economic correlations, *J. Membr. Sci.* **1** (1976), 49–63.
- [4] S. Loeb and R. S. Norman, Osmotic power plants, *Science* **189** (1975), no. 4203, 654–655.
- [5] R. S. Norman, Water salination: A source of energy, *Science* **186** (1974), no. 4161, 350–352.
- [6] A. Achilli and A. E. Childress, Pressure retarded osmosis: From the vision of Sidney Loeb to the first prototype installation – review, *Desalination* **261** (2010), no. 3, 205–211.
- [7] J. W. Post, J. Veerman, H. V. M. Hamelers, G. J. W. Euverink, S. J. Metz, K. Nymeijer, et al., Salinity-gradient power: Evaluation of pressure-retarded osmosis and reverse electrodialysis, *J. Membr. Sci.* **288** (2007), no. 1–2, 218–230.
- [8] F. Helfer, C. Lemckert and Y. G. Anissimov, Osmotic power with pressure retarded osmosis: Theory, performance and trends – A review, *J. Membr. Sci.* **453** (2014), 337–358.
- [9] K. L. Lee, R. W. Baker and H. K. Lonsdale, Membranes for power generation by pressure-retarded osmosis, *J. Membr. Sci.* **8** (1981), no. 2, 141–171.
- [10] K. Gerstandt, K. V. Peinemann, S. E. Skilhagen, T. Thorsen and T. Holt, Membrane processes in energy supply for an osmotic power plant, *Desalination* **224** (2008), no. 1–3, 64–70.
- [11] A. P. Straub, A. Deshmukh and M. Elimelech, Pressure-retarded osmosis for power generation from salinity gradients: Is it viable?, *Energy Environ. Sci.* **9** (2016), 31.
- [12] S. Lin, A. P. Straub and M. Elimelech, Thermodynamic limits of extractable energy by pressure retarded osmosis, *Energy Environ. Sci.* **7** (2014), no. 8, 2706–2714.
- [13] K. K. Reimund, J. R. McCutcheon and A. D. Wilson, Thermodynamic analysis of energy density in pressure retarded osmosis: The impact of solution volumes and costs, *J. Membr. Sci.* **487** (2015), 240.
- [14] S. Loeb, Large-scale power production by pressure-retarded osmosis, using river water and sea water passing through spiral modules, *Desalination* **143** (2002), no. 2, 115–122.
- [15] J. Kim, J. Lee and J. H. Kim, Overview of pressure-retarded osmosis (PRO) process and hybrid application to sea water reverse osmosis process, *Desalin. Water Treat.* **43** (2012), no. 1–3, 193–200.
- [16] C. F. Wan and T. S. Chung, Osmotic power generation by pressure retarded osmosis using seawater brine as the draw solution and wastewater brine as the feed, *J. Membr. Sci.* **479** (2015), 148–158.
- [17] K. Saito, M. Irie, S. Zaitzu, H. Sakai, H. Hayashi and A. Tanioka, Power generation with salinity gradient by pressure retarded osmosis using concentrated brine from SWRO system and treated sewage as pure water, *Desalin. Water Treat.* **41** (2012), no. 1–3, 114–121.
- [18] R. L. McGinnis, J. R. McCutcheon and M. Elimelech, A novel ammonia–carbon dioxide osmotic heat engine for power generation, *J. Membr. Sci.* **305** (2007), no. 1–2, 13–19.
- [19] S. Lin, N. Y. Yip, T. Y. Cath, C. O. Osuji and M. Elimelech, Hybrid pressure retarded osmosis–membrane distillation system for power generation from low-grade heat: Thermodynamic analysis and energy efficiency, *Environ. Sci. Technol.* **48** (2014), no. 9, 5306–5313.
- [20] G. Han, J. Zuo, C. F. Wan and T. S. Chung, Hybrid pressure retarded osmosis–membrane distillation (PRO–MD) process for osmotic power and clean water generation, *Environ. Sci. Water Res. Technol.* **1** (2015), 507–515.
- [21] G. Han, Q. C. Ge and T. S. Chung, Conceptual demonstration of novel closed-loop pressure retarded osmosis process for sustainable osmotic energy generation, *Appl. Energy* **132** (2014), 383–393.
- [22] M. F. Naguib, J. Maisonneuve, C. B. Laflamme and P. Pillay, Modeling pressure-retarded osmotic power in commercial length membranes, *Renew. Energy* **76** (2015), 619.
- [23] W. He, Y. Wang and M. H. Shaheed, Enhanced energy generation and membrane performance by two-stage pressure retarded osmosis (PRO), *Desalination* **359** (2015), 186–199.
- [24] A. P. Straub, S. Lin and M. Elimelech, Module-scale analysis of pressure retarded osmosis: Performance limitations and implications for full-scale operation, *Environ. Sci. Technol.* **48** (2014), no. 20, 12435–12444.
- [25] W. He, Y. Wang and M. H. Shaheed, Energy and thermodynamic analysis of power generation using a natural salinity gradient based pressure retarded osmosis process, *Desalination* **350** (2014), 86–94.

- [26] L. D. Banchik, M. H. Sharqawy and J. H. Lienhard, Limits of power production Due To finite membrane area in pressure retarded osmosis, *J. Membr. Sci.* **468** (2014), 81.
- [27] N. Y. Yip and M. Elimelech, Thermodynamic and energy efficiency analysis of power generation from natural salinity gradients by pressure retarded osmosis, *Environ. Sci. Technol.* **46** (2012), no. 9, 5230–5239.
- [28] A. Seppälä and M. J. Lampinen, Thermodynamic optimizing of pressure-retarded osmosis power generation systems, *J. Membr. Sci.* **161** (1999), no. 1–2, 115–138.
- [29] H. Struchtrup, *Thermodynamics and Energy Conversion*, Springer-Verlag, Heidelberg, 2014.
- [30] E. Michaelides, Entropy production and optimization of geothermal power plants, *J. Non-Eq. Thermodyn.* **37** (2012), no. 3, 233–246.
- [31] K. Wagner and K. H. Hoffmann, Endoreversible modeling of a PEM fuel cell, *J. Non-Eq. Thermodyn.* **40** (2015), no. 4, 283–294.
- [32] P. Geisler, W. Krumm and T. A. Peters, Reduction of the energy demand for seawater RO with the pressure exchange system PES, *Desalination* **135** (2001), no. 1–3, 205–210.
- [33] Y. Du, L. Xie, Y. Wang, Y. Xu and S. Wang, Optimization of reverse osmosis networks with spiral-wound modules, *Ind. Eng. Chem. Res.* **51** (2012), no. 36, 11764–11777.
- [34] G. Migliorini and E. Luzzo, Seawater reverse osmosis plant using the pressure exchanger for energy recovery: A calculation model, *Desalination* **165** (2004), 289–298.
- [35] V. G. Gude, Energy consumption and recovery in reverse osmosis, *Desalin. Water Treat.* **36** (2011), no. 1–3, 239–260.
- [36] Personal Communication, Rodney B. Clemente, VP, Technical Service & Aftermarket, Energy Recovery PX Device.
- [37] A. F. Mills, *Heat Transfer*, 2nd ed., Prentice Hall, Boston, 1998.
- [38] C. F. Wan and T. S. Chung, Energy recovery by pressure retarded osmosis (PRO) in SWRO–PRO integrated processes, *Appl. Energy* **162** (2016), 687–698.